16th European Signal Processing Conference (EUSIPCO 2008), Lausanne, Switzerland, August 25-29, 2008, copyright by EURASIP

ACCURATE PARAMETER ESTIMATION FOR AMPLITUDE MODULATED SINUSOIDAL SIGNALS INCORPORATING SMOOTHNESS CONSTRAINTS

S. Schuster, R. Feger, S. Scheiblhofer, and A. Stelzer

Institute for Communications and Information Engineering, Christian Doppler Laboratory for Integrated Radar Sensors,
University Linz, Altenbergerstr. 69, A-4040, Linz, Austria
phone: +43(0)732-2468-1822, fax: +43(0)732-2468-9712, email: s.schuster@icie.jku.at
web: www.icie.jku.at/cd-labor

ABSTRACT

Amplitude modulated sinusoidal signals arise in a wide variety of applications, e.g. in nuclear magnetic resonance spectroscopy [1], Doppler radar [2], and wide-band frequency-modulated continuous-wave radar signal processing. In some cases the type of amplitude modulation, e.g. exponential or polynomial, is known a priori, whereas in most practical cases such detailed information is not available. In this paper we derive estimators for the frequency, phase, and the modulation when only prior knowledge about the worst-case variation/smoothness of the modulation is available. No assumption on the type of modulation in terms of a parametric model is made. The estimators are compared to the best possible performance given by the Cramér-Rao lower bound (CRB) derived in [3]. Furthermore, they are shown to outperform the well-known “squaring loop” estimator [4, pp. 186], [5] that does not incorporate the smoothness of the modulation in terms of variance, threshold level (i.e. minimum necessary SNR for reliable operation), and restriction of the allowable range of signal frequencies in comparison to the sampling frequency. The presented method to incorporate constraints e.g. on the smoothness of the linear parameters in a parameter estimation problems with linear and nonlinear parameters is suitable to be applied in general constrained parameter estimation problems.

1. INTRODUCTION AND SIGNAL MODEL

In lots of applications, sinusoidal signals with a smooth deterministic amplitude modulation in noise are studied. Often, the only prior information available about the modulation is some knowledge of the minimum smoothness, obtained e.g. from simulation results or physical considerations. This prior information can be conveniently expressed e.g. through the worst-case (i.e. largest in magnitude) gradient and/or curvature of the modulation. To estimate the frequency and phase of the signal as accurately as possible, it is natural to try to incorporate the smoothness of the modulation into the estimators of the unknown parameters. In this paper it will be shown how this can be achieved and the benefit of doing so will be discussed.

Let the sampled complex data be

$$x[n] = s[n;\theta] + w[n] = a[n]\exp(\mathrm{j}(2\pi\psi_1 n + \phi_1)) + w[n], \quad (1)$$

with the vector of unknown parameters

$$\theta = [\, a[0] \;\; a[1] \;\; \cdots \;\; a[N-1] \;\; \phi_1 \;\; \psi_1 \,]^{\mathrm{T}},$$

and $n{=}0,1,\ldots,N-1$ (N is the number of samples), phase $-\pi \le \phi_1 < \pi$, normalized frequency $-1/2 \le \psi_1 < 1/2$. $w[n]$ denotes complex white Gaussian noise with variance σ^2. Nonlinear least squares (NLS) estimators for the case that $a[n] \in \mathbb{R}$ is an arbitrary real-valued envelope are known and given by ([4, pp. 186], [5])

$$\hat{\psi}_1^{(\mathrm{s})} = \arg\max_{\psi_1} \left| \sum_{n=0}^{N-1} x[n]^2 \exp(-\mathrm{j}4\pi\psi_1 n) \right| \quad (2)$$

$$\hat{\phi}_1^{(\mathrm{s})} = \frac{1}{2}\arctan\left(\frac{\mathrm{Im}\left\{ \sum_{n=0}^{N-1} x[n]^2 \exp\left(-\mathrm{j}4\pi\hat{\psi}_1^{(\mathrm{s})} n\right) \right\}}{\mathrm{Re}\left\{ \sum_{n=0}^{N-1} x[n]^2 \exp\left(-\mathrm{j}4\pi\hat{\psi}_1^{(\mathrm{s})} n\right) \right\}} \right) \quad (3)$$

$$\hat{a}[n]^{(\mathrm{s})} = \mathrm{Re}\left\{ x[n]\exp\left(-\mathrm{j}\left(2\pi\hat{\psi}_1^{(\mathrm{s})} n + \hat{\phi}_1^{(\mathrm{s})}\right)\right) \right\}. \quad (4)$$

$\mathrm{Re}\{\cdot\}$ and $\mathrm{Im}\{\cdot\}$ are the operators for taking the real and the imaginary part, respectively, and $\arg\max_x f(x)$ is the value of x that maximizes $f(x)$. Eq. (2) is often used in communications engineering e.g. for carrier recovery and is termed squaring loop (estimator). All results for the squaring loop estimators will be marked with a superscript (s), whereas all results for the newly derived estimator will be marked with a superscript (r). For the application of (2)-(4), it is necessary to restrict the normalized frequency to $-1/4 \le \psi_1 < 1/4$ due to the squaring operation. In [3], the authors derived the CRBs for the model (1). Regarding the frequency, it has been found that

$$\mathrm{CRB}_{\psi_1} = \mathrm{var}\{\hat{\psi}_1\} \ge \frac{\sigma^2}{8\pi^2} \frac{\sum_{n=0}^{N-1} a[n]^2}{\sum_{n=0}^{N-1} a[n]^2 n^2 \sum_{n=0}^{N-1} a[n]^2 - \left(\sum_{n=0}^{N-1} a[n]^2 n\right)^2} \quad (5)$$

is asymptotically achieved for high signal-to-noise ratio (SNR) by (2). In this paper, we concentrate on the case where the continuous-time modulation $a(t)$ has a bounded variation and/or smoothness, i.e. $\left|\partial a(t)/\partial t\right|$ and/or $\left|\partial^2 a(t)/\partial t^2\right|$ exist and are smaller than a priori known constants. To incorporate this prior information, we use a Tikhonov regularization approach together with the principle of separable least squares (LS), as shown next.

2. DERIVATIONS

2.1 Estimator

First, the model (1) can be written in matrix form as

$$\mathbf{x} = \mathbf{s} + \mathbf{w} = \mathbf{H}(\phi_1, \psi_1)\,\mathbf{a} + \mathbf{w},$$

where $\mathbf{a} {=} [\, a[0] \;\; a[1] \;\; \cdots \;\; a[N-1] \,]^{\mathrm{T}}$, $\xi[n] {=} \mathrm{j}(2\pi\psi_1 n + \phi_1)$, and

$$\mathbf{H}(\phi_1, \psi_1) = \mathrm{diag}\{ \exp(\xi[0]) \;\; \exp(\xi[1]) \;\; \cdots \;\; \exp(\xi[N-1]) \},$$

where $\mathrm{diag}\{\cdots\}$ denotes a diagonal matrix with entries $\{\cdots\}$ in its main diagonal. Note the nonlinear dependence of $\mathbf{s}$ on ϕ_1 and ψ_1 but the linear dependence on $\mathbf{a}$. Such a problem is called a separable LS problem in the literature [6], [7, pp. 256]. One possibility to incorporate the assumed prior knowledge on $\mathbf{a}$ is to use a (higher-order) Tikhonov regularization approach [8], [9, pp. 306], [10, pp. 89], where the following cost function is minimized:

$$J(\mathbf{a}, \phi_1, \psi_1) = \|\mathbf{x} - \mathbf{H}(\phi_1, \psi_1)\,\mathbf{a}\|_2^2 + \beta\|\Delta\mathbf{a}\|_2^2 + \gamma\|\Gamma\mathbf{a}\|_2^2. \quad (6)$$

In (6),

$$\Delta = \begin{bmatrix} -1 & 1 & 0 & \cdots & 0 & 0 \\ 0 & -1 & 1 & \ddots & \vdots & \vdots \\ 0 & 0 & \ddots & \ddots & 0 & 0 \\ \vdots & \ddots & \ddots & -1 & 1 & 0 \\ 0 & \cdots & 0 & 0 & -1 & 1 \end{bmatrix} \quad \Gamma = \begin{bmatrix} 1 & -2 & 1 & 0 & \cdots & 0 \\ 0 & 1 & -2 & 1 & \ddots & \vdots \\ \vdots & \ddots & \ddots & \ddots & \ddots & 0 \\ 0 & \cdots & 0 & 1 & -2 & 1 \end{bmatrix}$$

are approximate (scaled) differentiation and second-order differentiation operators, respectively, and $\|\cdot\|_2$ denotes the Euclidean norm. The real-valued regularization parameters $0 \leq \beta < \infty$ and $0 \leq \gamma < \infty$ are used to trade-off the objective $\|\mathbf{x} - \mathbf{Ha}\|_2^2$ and the variation/smoothness of the solution. For notational simplicity, we suppress the arguments of $\mathbf{H}$ from here on. Rewriting (6) as

$$J = (\mathbf{x} - \mathbf{Ha})^{\mathrm{H}} (\mathbf{x} - \mathbf{Ha}) + \mathbf{a}^{\mathrm{T}} \left(\beta \Delta^{\mathrm{T}} \Delta + \gamma \Gamma^{\mathrm{T}} \Gamma \right) \mathbf{a} \qquad (7)$$

and assuming that ϕ_1 and ψ_1 are known, it is straight forward to show that the minimizing solution for the modulation is

$$\hat{\mathbf{a}}^{(\mathrm{r})} = \left(\mathbf{I} + \beta \Delta^{\mathrm{T}} \Delta + \gamma \Gamma^{\mathrm{T}} \Gamma \right)^{-1} \mathrm{Re}\left\{ \mathbf{H}^{\mathrm{H}} \mathbf{x} \right\} = \mathbf{G} \mathrm{Re}\left\{ \mathbf{H}^{\mathrm{H}} \mathbf{x} \right\}. \quad (8)$$

$\mathbf{I}$ denotes the identity matrix, and we used the fact that $\mathbf{H}^{\mathrm{H}}\mathbf{H} = \mathbf{I}$, where the superscript H denotes transposition followed by complex conjugation. Note that $\hat{\mathbf{a}}$ still depends on ϕ_1 and ψ_1 through $\mathbf{H}$. To apply the principle of separable LS, we have to insert (8) back into (7), yielding the concentrated cost function

$$\begin{aligned} J'(\phi_1, \psi_1) \; &= \; \left(\mathbf{x} - \mathbf{HG} \mathrm{Re}\left\{ \mathbf{H}^{\mathrm{H}} \mathbf{x} \right\} \right)^{\mathrm{H}} \left(\mathbf{x} - \mathbf{HG} \mathrm{Re}\left\{ \mathbf{H}^{\mathrm{H}} \mathbf{x} \right\} \right) + \\ & \mathrm{Re}\left\{ \mathbf{H}^{\mathrm{H}} \mathbf{x} \right\}^{\mathrm{T}} \mathbf{G}^{\mathrm{T}} \underbrace{\left(\beta \Delta^{\mathrm{T}} \Delta + \gamma \Gamma^{\mathrm{T}} \Gamma \right)}_{\mathbf{K}} \mathbf{G} \mathrm{Re}\left\{ \mathbf{H}^{\mathrm{H}} \mathbf{x} \right\}. \end{aligned}$$

Expanding above equation yields, after some straight forward manipulations,

$$\begin{aligned} J'(\phi_1, \psi_1) \; &= \; \mathbf{x}^{\mathrm{H}} \mathbf{x} - 2 \mathrm{Re}\left\{ \mathbf{x}^{\mathrm{H}} \mathbf{H} \right\} \mathbf{G} \mathrm{Re}\left\{ \mathbf{H}^{\mathrm{H}} \mathbf{x} \right\} + \\ & \mathrm{Re}\left\{ \mathbf{x}^{\mathrm{H}} \mathbf{H} \right\} \mathbf{G}^2 \mathrm{Re}\left\{ \mathbf{H}^{\mathrm{H}} \mathbf{x} \right\} + \mathrm{Re}\left\{ \mathbf{H}^{\mathrm{H}} \mathbf{x} \right\}^{\mathrm{T}} \mathbf{GKG} \mathrm{Re}\left\{ \mathbf{H}^{\mathrm{H}} \mathbf{x} \right\}. \end{aligned}$$

We used the facts that $\mathbf{H}^{\mathrm{H}}\mathbf{H} = \mathbf{I}$, $\mathbf{G}^{\mathrm{T}} = \mathbf{G}$, and

$$\mathrm{Re}\left\{ \mathbf{x}^{\mathrm{H}} \mathbf{H} \right\} \mathbf{G} \mathbf{H}^{\mathrm{H}} \mathbf{x} + \mathbf{x}^{\mathrm{H}} \mathbf{HG} \mathrm{Re}\left\{ \mathbf{H}^{\mathrm{H}} \mathbf{x} \right\} = 2 \mathrm{Re}\left\{ \mathbf{x}^{\mathrm{H}} \mathbf{H} \right\} \mathbf{G} \mathrm{Re}\left\{ \mathbf{H}^{\mathrm{H}} \mathbf{x} \right\}.$$

Grouping common terms leads to

$$\begin{aligned} J'(\phi_1, \psi_1) \; &= \; \mathbf{x}^{\mathrm{H}} \mathbf{x} - \mathrm{Re}\left\{ \mathbf{x}^{\mathrm{H}} \mathbf{H} \right\} \mathbf{G} [2\mathbf{I} - \mathbf{G} - \mathbf{KG}] \mathrm{Re}\left\{ \mathbf{H}^{\mathrm{H}} \mathbf{x} \right\} \\ &= \; \mathbf{x}^{\mathrm{H}} \mathbf{x} - \mathrm{Re}\left\{ \mathbf{x}^{\mathrm{H}} \mathbf{H} \right\} \mathbf{G} [2\mathbf{I} - (\mathbf{I} + \mathbf{K}) \mathbf{G}] \mathrm{Re}\left\{ \mathbf{H}^{\mathrm{H}} \mathbf{x} \right\}. \end{aligned}$$

With $\mathbf{I} + \mathbf{K} = \mathbf{G}^{-1}$ we obtain

$$J'(\phi_1, \psi_1) = \mathbf{x}^{\mathrm{H}} \mathbf{x} - \mathrm{Re}\left\{ \mathbf{x}^{\mathrm{H}} \mathbf{H} \right\} \mathbf{G} \mathrm{Re}\left\{ \mathbf{H}^{\mathrm{H}} \mathbf{x} \right\}.$$

To minimize above cost function, we can equivalently maximize

$$\begin{aligned} J''(\phi_1, \psi_1) \; &= \; \mathrm{Re}\left\{ \mathbf{x}^{\mathrm{H}} \mathbf{H} \right\} \mathbf{G} \mathrm{Re}\left\{ \mathbf{H}^{\mathrm{H}} \mathbf{x} \right\} \\ &= \; \sum_{k=0}^{N-1} \sum_{n=0}^{N-1} g[n,k] \, \mathrm{Re}\{ x[k]^* \exp(\mathrm{j}2\pi \psi_1 k + \mathrm{j}\phi_1) \} \\ & \times \; \mathrm{Re}\{ x[n] \exp(-\mathrm{j}2\pi \psi_1 n - \mathrm{j}\phi_1) \}, \end{aligned}$$

where $g[n,k] = [\mathbf{G}]_{nk}$, i.e. $g[n,k]$ is the nkth element of $\mathbf{G}$, and the superscript $*$ denotes complex conjugation. After applying some standard trigonometric identities and further simplification, we finally obtain the following estimators:

$$\hat{\psi}_1^{(\mathrm{r})} = \arg\max_{\psi_1} \left| \sum_{k=0}^{N-1} \sum_{n=0}^{N-1} g[n,k] \, x[n] \, x[k] \exp(-\mathrm{j}2\pi \psi_1 (n+k)) \right| \quad (9)$$

$$\hat{\phi}_1^{(\mathrm{r})} = \frac{1}{2} \arg \sum_{k=0}^{N-1} \sum_{n=0}^{N-1} g[n,k] \, x[n] \, x[k] \exp(-\mathrm{j}2\pi \hat{\psi}_1 (n+k)) \, . (10)$$

$\arg\{\cdot\}$ denotes the argument operator. Using (9) and (10), (8) can be rewritten to

$$\hat{a}[n]^{(\mathrm{r})} = \sum_{k=0}^{N-1} g[n,k] \, \mathrm{Re}\left\{ x[k] \exp\left(-\mathrm{j}2\pi \hat{\psi}_1^{(\mathrm{r})} k - \mathrm{j}\hat{\phi}_1^{(\mathrm{r})} \right) \right\}. \qquad (11)$$

As a first verification, consider the case of no prior knowledge, i.e. $\beta \to 0$, $\gamma \to 0$. In this case, $\mathbf{G} = \mathbf{I}$, or $g[n,k] = 0$ for all $n \neq k$ and 1 otherwise. Hence, (9) can be rewritten as

$$\hat{\psi}_1^{(\mathrm{r})} \Big|_{\substack{\beta \to 0 \\ \gamma \to 0}} = \arg\max_{\psi_1} \left| \sum_{n=0}^{N-1} x[n]^2 \exp(-\mathrm{j}4\pi \psi_1 n) \right|.$$

But this is exactly (2), and hence the derived estimator (9) coincidences with the squaring loop estimator in case of no prior knowledge, as expected.

It should be noted that the used approach to incorporate prior knowledge in NLS problems is not limited to solve the here presented problem, but is applicable in a quite wide variety of applications. Also, the principle is by no means restricted to Tikhonov regularization only. In fact, constrained estimation is an active topic of research, and significant advances have been achieved in recent years, see e.g. the papers of Eldar [11,12] and Benavoli et al. [13,14]. These methods can be used alternatively. Also other types of prior information can be incorporated. However, the presented approach significantly improves the performance of the estimators compared to the non-regularized case, as we will show. Furthermore, it can be efficiently implemented, as $\mathbf{G}$ can be computed offline, so that no matrix inversion etc. is required. Before proceeding by presenting some expressions for the large-sample variances of the derived estimators in comparison to the squaring loop estimator and discussing how to choose β and γ, it is advisable to point out some facts about the matrix $\mathbf{G}$. As Δ is bidiagonal and Γ is tridiagonal with equal elements in each diagonal, we can expect $\mathbf{G}$ to be highly structured. In fact, it is found additionally to the symmetry of $\mathbf{G}$ that all elements of a diagonal of $\mathbf{G}$ are nearly equal. Only the first and last few elements in every diagonal are slightly different due to "edge effects" when applying the derivative operations. Furthermore, it is found that—depending on the choice of β and γ—the first few sub- and superdiagonals are significantly larger than the remaining sub- and superdiagonals. This will be exploited in Subsection 2.3 to derive a computationally efficient implementation of (9).

2.2 Bias and Variance Expressions, CRB

First, an expression for the bias and variance of the squaring loop estimator (2) should be derived. In principle, a standard Taylor-series expansion approach can be used to assess expressions for the bias and variance of (2) for large N. However, we can greatly simplify the derivation and gain further insight by expanding (2) in the following way

$$\begin{aligned} \hat{\psi}_1^{(\mathrm{s})} \; &= \; \arg\max_{\psi_1} \left| \sum_{n=0}^{N-1} x[n]^2 \exp(-\mathrm{j}4\pi \psi_1 n) \right| \\ &= \; \arg\max_{\psi_1} \left| \sum_{n=0}^{N-1} \left(s[n]^2 + 2w[n] \, s[n] + w[n]^2 \right) \exp(-\mathrm{j}4\pi \psi_1 n) \right|. \end{aligned}$$

The idea is now to express $x[n]^2 = x'[n]$, i.e. $s[n]^2 + 2w[n]s[n] + w[n]^2 = s'[n] + w'[n]$. Thus, we represent the squared data through a modified mean and additive noise with a certain covariance matrix. Proceeding this way, we can rewrite (2) to

$$\hat{\psi'}_1^{(\mathrm{s})} = \arg\max_{\psi'_1} \left| \sum_{n=0}^{N-1} x'[n] \exp\left(-\mathrm{j}2\pi\psi'_1 n\right) \right|,$$

where $\psi'_1 = 2\psi_1$, $\phi'_1 = 2\phi_1$, and $s'[n] = a[n]^2 \exp\left(\mathrm{j}2\pi\psi'_1 n\right)\exp\left(\mathrm{j}\phi'_1\right)$. Above equation is equivalent to a standard discrete Fourier transform (DFT) magnitude spectrum frequency estimator, but with modified data $x'[n]$. It can be easily shown that $w'[n] = 2w[n]s[n] + w[n]^2$ has zero mean and its covariance matrix is given by

$$\mathbf{C}_{\mathbf{w}'\mathbf{w}'} = 4\sigma^2 \mathrm{diag}\left\{ \frac{\sigma^2}{2} + a[0]^2 \;\; \frac{\sigma^2}{2} + a[1]^2 \;\; \cdots \;\; \frac{\sigma^2}{2} + a[N-1]^2 \right\}.$$

Due to the squaring operation, the covariance matrix is both a function of σ^2 and σ^4. The reason is that the squaring loop estimator has a built-in estimator for $a[n]$ to weight the data according to the SNR of each individual sample, as noted in [3], with variance $\sigma^2/2$. We can now directly apply the results presented in [3] for the standard DFT frequency estimator in case of amplitude modulated data and obtain $\mathrm{bias}\left\{\hat{\psi}_1^{(\mathrm{s})}\right\} \approx 0$ and

$$\mathrm{var}\left\{\hat{\psi}_1^{(\mathrm{s})}\right\} = \frac{1}{4}\mathrm{var}\left\{\hat{\psi'}_1^{(\mathrm{s})}\right\}$$
$$\approx \frac{\sigma^2}{8\pi^2} \frac{\sum_{m=0}^{N-1}\left(\frac{\sigma^2}{2} + a[m]^2\right)\left(\sum_{n=0}^{N-1} a[n]^2 n - m\sum_{n=0}^{N-1} a[n]^2\right)^2}{\left[\left(\sum_{n=0}^{N-1} a[n]^2 n\right)^2 - \left(\sum_{n=0}^{N-1} a[n]^2 n^2\right)\left(\sum_{n=0}^{N-1} a[n]^2\right)\right]^2}. \quad (12)$$

It is interesting to examine the high SNR case $\sigma^2/2 \ll a[m]^2$. By expanding the numerator of (12), simplification and comparison with (5) it follows that

$$\mathrm{var}\left\{\hat{\psi}_1^{(\mathrm{s})}\right\}\Big|_{\sigma^2/2 \ll a[m]^2} \rightarrow \mathrm{CRB}_{\psi_1}.$$

This result is not surprising, as at high SNR the squaring loop estimator should attain the derived CRB whereas at moderate and low SNR the built-in estimate of the modulation effectively introduces a further increase in estimation variance.

For the regularized estimator, we first discuss the estimator of the modulation. It is straightforward to show that $\mathrm{bias}\{\hat{\mathbf{a}}\} \approx (\mathbf{G} - \mathbf{I})\mathbf{a}$ and $\mathbf{C}_{\hat{\mathbf{a}}\hat{\mathbf{a}}} \approx \frac{\sigma^2}{2}\mathbf{G}^2$, where $\mathbf{C}_{\hat{\mathbf{a}}\hat{\mathbf{a}}}$ is the covariance matrix of $\hat{\mathbf{a}}$. Written for each individual element of $\hat{\mathbf{a}}$, we have

$$\mathrm{bias}\left\{\hat{a}[n]^{(\mathrm{r})}\right\} \approx \sum_{r=0}^{N-1} g[n,r]\,a[r] - a[n] \quad (13)$$

and

$$\mathrm{var}\left\{\hat{a}[n]^{(\mathrm{r})}\right\} \approx \frac{\sigma^2}{2}\bar{g}_n \quad (14)$$

where $\bar{g}_n = \sum_{r=0}^{N-1} g[n,r]^2$. We found that $\mathrm{bias}\left\{\hat{\psi}_1^{(\mathrm{r})}\right\} \approx 0$ and

$$\mathrm{var}\left\{\hat{\psi}_1^{(\mathrm{r})}\right\} \approx$$
$$\frac{\sigma^2}{8\pi^2} \frac{\sum_{m=0}^{N-1}\left(\frac{\sigma^2}{2}\bar{g}_n + a[m]^2\right)\left(\sum_{n=0}^{N-1} a[n]^2 n - m\sum_{n=0}^{N-1} a[n]^2\right)^2}{\left[\left(\sum_{n=0}^{N-1} a[n]^2 n\right)^2 - \left(\sum_{n=0}^{N-1} a[n]^2 n^2\right)\left(\sum_{n=0}^{N-1} a[n]^2\right)\right]^2} \quad (15)$$

for suitable choices of β and γ as discussed later. This sheds light on the operational principle of the estimator. By comparing (12) with (15) we see that the only difference is that $\bar{g}_n$ appears in the numerator of (15). Thus, the prior knowledge is incorporated in (15) simply by an improved estimate of the modulation. In fact, if β and γ are suitably chosen, $\mathrm{mse}\left\{\hat{a}[n]^{(\mathrm{r})}\right\} \approx \mathrm{var}\left\{\hat{a}[n]^{(\mathrm{r})}\right\} \approx \frac{\sigma^2}{2}\bar{g}_n$ for low and moderate SNRs, i.e. high σ^2, $\mathrm{mse}\{\cdot\}$ denotes the mean-square error (MSE). Hence, the variance of the estimate will be decreased compared to the squaring loop estimator, because $\bar{g}_n < 1$ for all $\beta > 0$ and/or $\gamma > 0$. On the other hand, for high SNR, the variance of the estimates should be nearly equal. Similar results for the phase estimator (10) can be obtained.

2.3 Computationally Efficient Implementation

As already stated and depending on the choice of β and γ, most sub- and superdiagonals of $\mathbf{G}$ are significantly smaller than a few diagonals located near the main diagonal, i.e $g[n,k] \approx 0$ for $|n-k| > d$. This enables us to rewrite (9) in the approximate form

$$\hat{\psi}_1^{(\mathrm{r})} \approx \arg\max_{\psi_1} \left| \sum_{n=0}^{N-1} g[n,n]\,x[n]^2 \exp(-\mathrm{j}4\pi\psi_1 n) + \right.$$
$$\sum_{k=1}^{d}\left[\exp(-\mathrm{j}2\pi\psi_1 k)\sum_{n=0}^{N-1-k} g[n,n+k]\,x[n]\,x[n+k]\exp(-\mathrm{j}4\pi\psi_1 n) + \right.$$
$$\left.\left. \exp(+\mathrm{j}2\pi\psi_1 k)\sum_{n=k}^{N-1} g[n,n-k]\,x[n]\,x[n-k]\exp(-\mathrm{j}4\pi\psi_1 n)\right]\right|. \quad (16)$$

Note that every sum in (16) can be efficiently implemented using a fast Fourier transform (FFT) algorithm and zeropadding. Hence the overall computational complexity of the algorithm is reduced from $\mathscr{O}\left(N^2\log(N)\right)$ to $\mathscr{O}(dN\log(N))$, $\mathscr{O}$ denoting the Landau symbol. In most practical cases, $d \ll N$ can be used depending on the choice of β and γ, resulting in a significantly reduced computational burden of the overall algorithm. More precise expressions how to choose d as a function of β, γ, and N and the associated increase in variance of the estimates are subject of future work. However, in most cases even without this approximate realization, (9) should be competitive from a computational complexity point of view to estimators that are based on a parametric model of the envelope. Furthermore, above representation also reveals another feature of (9). As the estimator now not only acts on the squared data, but also uses products of samples which are lagged to each other as long as $\beta > 0$ and/or $\gamma > 0$, the restriction of the allowable range of frequencies for the squaring loop estimator $-1/4 \leq \psi_1 < 1/4$ can be changed to the usual range $-1/2 \leq \psi_1 < 1/2$. In Section 3 an example is shown that illustrates this behavior.

2.4 Choice of Regularization Parameters

For application of above described algorithm, a method for choosing β and γ is necessary.

First we discuss the case that a prototype signal with the worst-case modulation $a[n]$ is available, e.g. from a simulation result. Now, because the estimator utilizes a built-in estimate of the modulation, it is natural to choose β and γ in such a way so that the estimator of the modulation—evaluated at the true frequency and phase—performs well in terms of MSE for the SNRs of interest. Several methods for choosing the desired parameters for this linear parameter estimation problem are known, e.g. the L-Curve method or generalized cross validation, see e.g. [10].

On the other hand, if only the worst-case gradient and/or curvature is known, another approach is necessary. We found empirically that

$$\beta = \frac{1}{f_\mathrm{s}\max_t\left\{\left|\frac{\partial a(t)}{\partial t}\right|\right\}} \qquad \gamma = \frac{1}{f_\mathrm{s}^2\max_t\left\{\left|\frac{\partial^2 a(t)}{\partial t^2}\right|\right\}} \quad (17)$$

should be chosen for a good performance, with f_s the sampling frequency. Further improvement might be obtained by incorporating the SNR in above formulas. However, this prevents the algorithm from being applicable for $-1/2 \leq \psi_1 < 1/2$ instead of $-1/4 \leq \psi_1 < 1/4$, because for increasing SNR the regularization would be more and more suppressed, and for $\sigma^2 \to 0$, no regularization will be present, leading to the squaring loop estimator with its restricted range for the signal's frequency.

3. SIMULATION RESULTS

To validate the presented algorithms and formulas, we performed Monte Carlo simulations with 10^4 trials for each SNR for a complex sinusoidal signal with $N=128$, $\psi_1=0.125$, $\phi_1=\pi/2$, sampling frequency $f_s=1$ and various envelopes as shown in Fig. 1. For brevity, we concentrate on the frequency only. As our worst-case scenario in terms of variation and smoothness, we defined $\max_t \left| \partial a(t) / \partial t \right| = 0.1$ and $\max_t \left| \partial^2 a(t) / \partial t^2 \right| = 0.01$. Using the approach described in Subsection 2.4, we found $\beta=10$ and $\gamma=100$ from (17), which have been subsequently used for all simulations to compare the performance of the algorithms also if some of the signals under test have in fact much lower gradient and curvature values. In all simulations, we used the efficient implementation (16) of the regularized estimator with $d=15$ and sufficient zero-padding to avoid discretization effects of the frequency axis. For this choice of d only a negligible increase of the MSE in comparison to the full solution (9) has been observed. The SNR has been defined as $\eta = 10\log_{10}\left(1/\sigma^2\right)$. In Fig. 2, a simulation for a relatively moderate exponential modulation $a(t) = \exp(-0.03t)$ ("modulation 1" in Fig. 1) is shown. The frequency estimates obtained from the regularized estimator have lower root mean square error (RMSE) than the estimates obtained from the squaring loop estimator, especially for low and moderate SNRs. At high SNR, both estimators perform equally. Furthermore, the threshold level, i.e. the level of minimum necessary SNR for reliable operation, is much lower for the regularized estimator. Also the derived RMSE predictions (12) and (15) are in good agreement with the simulation results above threshold. For comparison purposes, we also show results for the maximum likelihood estimator (MLE) derived in [3] when the modulation is known, together with the corresponding CRLB (5). The latter can be considered as a benchmark for all other estimators. Also results when applying the standard DFT magnitude spectrum frequency estimator are shown, underlining the good performance of the regularized estimator. Note that the difference in RMSE between the squaring loop estimator and the other estimators at very low SNR results from the different restrictions of the allowable ranges of frequencies. In Fig. 3, the exponential envelope $a(t) = \exp(-0.1t)$ ("modulation 2" in Fig. 1) is used, which is an example for the worst-case scenario defined. Also here, the regularized estimator significantly outperforms both the squaring loop estimator and the standard DFT magnitude spectrum based estimator, and its RMSE is near to the RMSE of the MLE for known modulation. The absolute levels of the threshold change from "modulation 1" to "modulation 2" because the energy $\sum_{n=0}^{N-1} a[n]^2$ is different for different modulations, which has intentionally not been incorporated in the used SNR definition to show the effect.

All estimators except the MLE for known modulation show an interesting RMSE behavior for moderate SNRs, which is not predicted by the expressions developed in Subsection 2.2. The reason for this behavior is that for strong modulations and low SNRs, the cost functions become non-quadratically near the true value of the parameters, making the used Taylor-series expansion approaches for deriving the RMSE predictions invalid. In Fig. 4, results for a bell-shaped modulation ("modulation 3" in Fig. 1) are shown, with worst-case derivative and curvature in between "modulation 1" and "modulation 2". The results once again show the good performance of the regularized estimator. Fig. 5 shows results if no modulation is present. The decreased threshold level of the regularized estimator can clearly be seen.

Finally, in Fig. 6 a comparison between the cost function maximized by the squaring loop estimator, by the regularized estimator, and by the approximate realization of the latter for $a(t) = \exp(-0.1t)$ and high SNR is depicted. Clearly, the regularized estimator has only one global maximum in the range $-1/2 \leq \psi_1 < 1/2$ in contrast to the squaring loop estimator, as discussed. Also the effect of retaining only the first d diagonals in the approximate realization as a slight increase of the cost function especially near the second global maximum of the squaring loop estimator can be observed.

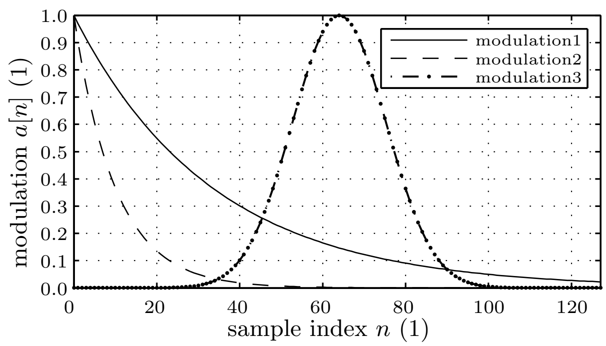

Figure 1: Different modulations used in the Monte Carlo simulations.

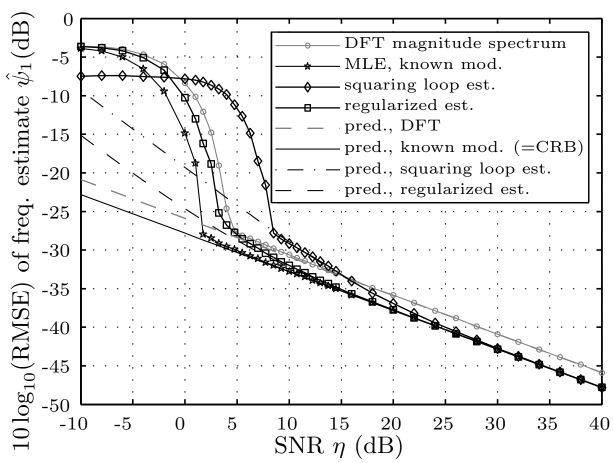

Figure 2: Simulation results for "modulation 1" (a weak exponential modulation). The results clearly show the decreased threshold level and decreased MSE of the regularized estimator in comparison to the squaring loop estimator.

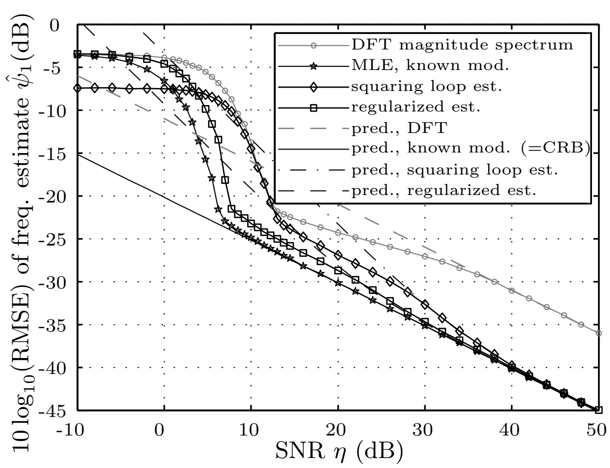

Figure 3: Simulation results for "modulation 2" (a strong exponential modulation).

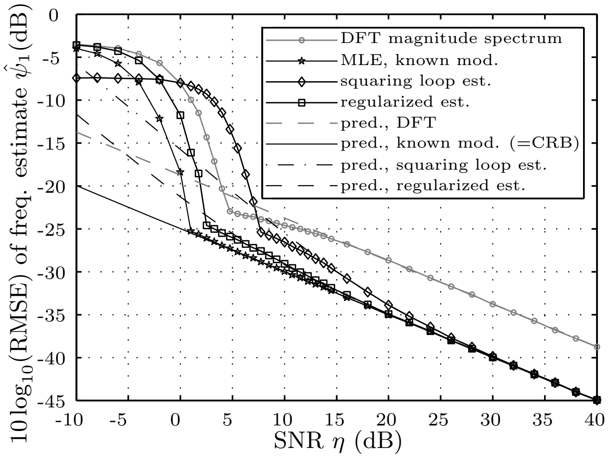

Figure 4: Simulation results for "modulation 3" (a bell-shaped modulation).

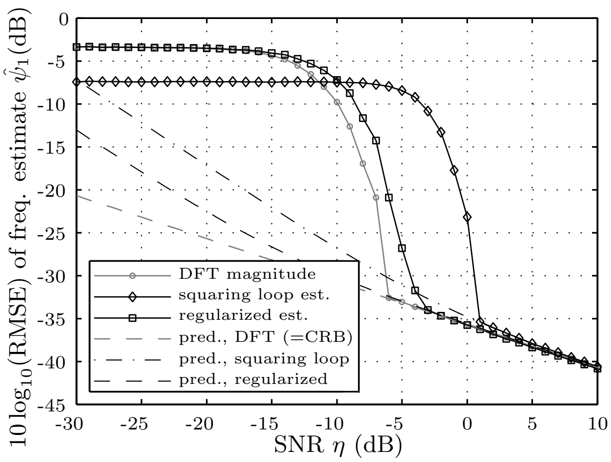

Figure 5: Simulation results if no modulation is present. Also here, the regularized estimator performs better than the squaring loop estimator in terms of a decreased threshold level.

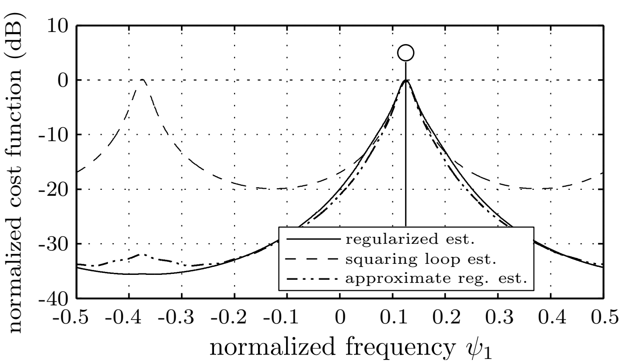

Figure 6: Plot of the cost functions for the squaring loop, the regularized, and the efficiently implemented regularized estimator at high SNR. The true frequency is marked. It can be clearly seen that in contrast to the squaring loop estimator the (efficiently implemented) regularized estimator does not suffer from a second global maximum if $-1/2 \leq \psi_1 < 1/2$ is chosen as the valid range for signal frequencies.

4. CONCLUSION

We presented new algorithms for estimating the phase, frequency, and modulation of a sinusoidal waveform with deterministic amplitude modulation. One strength of the presented algorithm is that the prior knowledge of worst-case smoothness/variation is incorporated in a computationally efficient manner, without the necessity of specifying any parametric model of the envelope. This renders the algorithm useful in a wide variety of applications without modification. In contrast, commonly used algorithms that rely on a particular model of the envelope may perform poorly if the true modulation does not match the assumed one. Furthermore, it has been shown that the algorithms outperform an existing set of squaring loop algorithms both in terms of estimation variance and threshold level. For the application of the squaring loop algorithms the frequency of the sinusoidal signal needs to be restricted to one quarter of the sampling frequency, instead of the usual one half of the sampling frequency. This restriction is not necessary for the application of the presented algorithm.

REFERENCES

[1] G. L. Bretthorst, *Bayesian Spectrum Analysis and Parameter Estimation*, ser. Lecture Notes in Statistics. Springer, 1988.

[2] M. Ghogho, A. Swami, and T. S. Durrani, "Frequency estimation in the presence of doppler spread: Performance analysis," *IEEE Trans. Signal Processing*, vol. 49, no. 4, pp. 777–789, Apr. 2001.

[3] S. Schuster, S. Scheiblhofer, and A. Stelzer, "Parameter Estimation for Sinusoidal Signals with Deterministic Amplitude Modulation," in *15th European Signal Processing Conference*, Poznan, Poland, Sept. 3-7 2007.

[4] P. Stoica and R. Moses, *Spectral Analysis of Signals*. Englewood Cliffs, Upper Saddle River, NJ: Prentice Hall, 2005.

[5] O. Besson and P. Stoica, "Nonlinear Least-Squares Frequency Estimation and Detection for Sinusoidal Signals with Arbitrary Envelope," *Tech. Rep 97 093R, Uppsala University*, 1997.

[6] G. H. Golub and V. Pereyra, "The Differentiation of Pseudoinverses and Nonlinear Least Squares Problems whose Variables Separate," *SIAM J. Numer. Anal.*, no. 10, pp. 413–432, 1973.

[7] S. M. Kay, *Fundamentals of Statistical Signal Processing-Estimation Theory*. Englewood Cliffs, Upper Saddle River, NJ: Prentice Hall, 1993.

[8] A. N. Tikhonov and V. Y. Arsenin, *Solutions of Ill-Posed Problems*. V. H. Winston and Sons, 1977 (Translated from Russian).

[9] S. Boyd and L. Vandenberghe, *Convex Optimization*. Cambridge University Press, 2004.

[10] R. C. Aster and B. B. C. H. Thurber, *Parameter Estimation and Inverse Problems*. Elsevier Academic Press, 2004.

[11] Y. C. Eldar, "Uniformly Improving the Cramér-Rao Bound and Maximum-Likelihood Estimation," *IEEE Trans. Signal Processing*, vol. 54, no. 8, pp. 2943–2956, Aug. 2006.

[12] ——, "Minimum Variance in Biased Estimation: Bounds and Asymptotically Optimal Estimators," *IEEE Trans. Signal Processing*, vol. 52, no. 7, pp. 1915–1930, Oct. 2004.

[13] A. Benavoli, L. Chisci, and A. Farina, "Estimation of Constrained Parameters With Guaranteed MSE Improvement," *IEEE Trans. Signal Processing*, vol. 55, no. 4, pp. 1264–1274, Apr. 2007.

[14] A. Benavoli, L. Chisci, A. Farina, L. Ortenzi, and G. Zappa, "Hard-Constrained versus Soft-Constrained Parameter Estimation," *IEEE Trans. Aerosp. Elect. Syst.*, vol. 42, no. 4, pp. 1224–1239, Oct. 2006.